The Evolution of Dynamical Screening in the Parton Cascade Model

Helmut Satz[1] and Dinesh Kumar Srivastava[1,2]

1: Fakultät für Physik, Universität Bielefeld, D-33501 Bielefeld, Germany

2: Variable Energy Cyclotron Centre, 1/AF Bidhan Nagar, Calcutta 700 064, India

Abstract

We determine the time evolution of the colour screening mass in high energy nuclear collisions, as provided by the parton cascade model. Using our result, we discuss the onset of deconfinement and the onset of quarkonium suppression in a general, not necessarily equilibrated environment of strongly interacting constituents.

Statistical QCD predicts that with increasing temperature, strongly interacting media will undergo a transition from hadronic matter to quark-gluon plasma. The aim of high energy nuclear collisions is to study this transition and the resulting new deconfined phase in the laboratory. However, statistical QCD deals with large systems in thermal equilibrium, while nuclear collisions provide small, rapidly evolving systems. A study of the onset of deconfinement in a microscopic, non-equilibrium space-time picture would therefore be of great help in understanding if and to what extent theory and experiment can be expected to meet. The aim of the parton cascade model [1, 2] is to describe the evolution of a high energy nucleus-nucleus collision through perturbative partonic interactions embedded in a relativistic transport theory. Hence it seems to be a good starting point for a 'dynamic study of deconfinement'.

The initial state of two colliding nucleons can be pictured as colliding beams of confined partons. The incident partons have a distribution in intrinsic transverse momentum, leading to some average value $\langle k_T \rangle$, which in turn defines an average transverse parton size $r_T = 1/\langle k_T \rangle$. When two nuclei collide at high energy, the transverse parton density increases considerably, since now we have a superposition of nucleon-nucleon collisions. In this medium, colour screening will destroy the association of partons to particular hadrons, since for a sufficiently high density of colour charges, the colour screening radius becomes much smaller than the typical hadronic scale. Hence we expect the onset of deconfinement for some characteristic density or for an equivalent screening scale. In perturbative QCD, the method to calculate the colour screening mass μ (the inverse of the screening radius r_D) is well-known; an extension to the non-equilibrium medium provided by cascade models has also been proposed [3, 4]. We shall therefore use this method to obtain the time evolution of the screening mass $\mu(t)$ in the parton cascade model.

Given $\mu(t)$, we have to specify for what value deconfinement sets in; the parton cascade model itself does not identify such a point. It just has the primary collisions between the 'confined' partons of the incident nucleons, followed by successive interactions between primary as well as produced partons and eventually by the hadronisation of partons according to some assumed scheme. There are two possible ways to specify deconfinement in such a picture. One can obtain at any given time the transverse density profile of the parton distribution, and use the percolation point of partonic discs in the transverse plane to define the onset of deconfinement [5]–[7]. Here we shall follow a somewhat different path, taking as critical screening mass μ_c the value obtained from lattice studies. These provide the temperature dependence of μ and in particular also its value at the deconfinement point T_c, where one has $\mu_c \equiv \mu(T_c) \simeq 0.4 - 0.6$ GeV [8]. It is not obvious that such an equilibrium value is really applicable to the non-equilibrium situation provided by the parton cascade model. A good check would be to compare in this model the transverse parton density at μ_c to the percolation value. Work on this is in progress.

Let us briefly recall the most important features of the parton cascade model.

- The initial nucleus-nucleus system is treated as two colliding clouds of partons, whose distributions are fixed by the nucleonic parton distribution functions determined in deep inelastic lepton-nucleon scattering, and by the nucleon density distributions in the nuclei.

- The parton cascade development starts when the initial parton clouds interpenetrate, and it follows their space-time development due to interactions. The model includes multiple elastic and inelastic interactions described as sequences of $2 \rightarrow 2$ scatterings, $1 \rightarrow 2$ emissions, and $2 \rightarrow 1$ fusions. It moreover explicitly accounts for the individual time scale of each parton-parton collision, the formation time of the parton radiation, the effective suppression of radiation from virtual partons due to an enhanced absorption probability by others in regions of dense phase space occupation, and the effect of soft gluon interference in low energy gluon emission.

- Finally, the hadronization in terms of a parton coalescence to colour neutral clusters is described as a local statistical process that depends on the spatial separation and colour of the nearest-neighbour partons [9]. These pre-hadronic clusters then decay to form hadrons.

Since we are interested in the early state of the collision when the strongly interacting matter is still in partonic form, the hadronisation part of the model will not play a role for our considerations.

To specify the further basis for our considerations, we add some details of the parton-parton scattering considered in the parton cascade model [1, 2]. The elementary parton scatterings $a + b \rightarrow c + d$ and the fusion processes $a + b \rightarrow c^*$ themselves are devided into two distinct classes:

i) *hard* parton collisions with a sufficiently large momentum transfer $p_\perp^2$ or invariant mass $\hat{s}$ to apply perturbative QCD; and

ii) *soft* parton collisions with low momentum transfer $p_\perp^2$ or invariant mass $\hat{s}$, which will be modelled phenomenologically.

This division is necessary to regulate the collision integrals which appear in the transport equations describing the evolution of the partonic system and which are singular for small momentum transfer Q^2 in the Born approximation. The parton-parton cross-section is rendered finite by invoking an invariant *hard-soft division scale* p_0^2 such that the collisions occuring at a momentum scale $Q^2 \geq p_0^2$ are treated perturbatively, whereas a soft, non-perturbative interaction is assumed for those with $Q^2 < p_0^2$. The total cross-section for collisions between two partons is then written as

$$\widehat{\sigma}_{ab}(\widehat{s}) = \sum_{c,(d)} \left\{ \int_0^{p_0^2} dQ^2 \left(\frac{d\widehat{\sigma}_{ab\to c(d)}^{soft}}{dQ^2} \right) + \int_{p_0^2}^{\widehat{s}} dQ^2 \left(\frac{d\widehat{\sigma}_{ab\to c(d)}^{hard}}{dQ^2} \right) \right\} , \tag{1}$$

where the symbols have their usual meaning. The specific value of p_0 is fixed by demanding that the energy dependence of the total cross-section for *pp* collisions is correctly reproduced when the expression is convoluted with the structure function of the nucleons within an eikonal approximation [2]. One way to satisfy this requirement is a scale [10]

$$p_0 \equiv p_0(\sqrt{s}) = 0.5(\sqrt{s})^{0.27} \tag{2}$$

and we shall use this form, where $\sqrt{s}$ is the nucleon-nucleon c.m.s. energy.

In the two-term Ansatz (1), the hard and soft contributions now have to be specified. For the hard collisions above p_0 we use the standard form

$$\frac{d\widehat{\sigma}_{ab\to cd}^{hard}}{dQ^2} = \frac{1}{16\pi\widehat{s}^2}|\overline{M}_{ab\to cd}(\widehat{s}, Q^2)|^2 \sim \frac{\pi\alpha_s^2(Q^2)}{Q^2} \tag{3}$$

where $|M|^2$ is the process-dependent spin- and colour-averaged squared matrix element in Born approximation. To account for higher order contributions, we modify the corresponding cross sections by a K-factor of 2.5 [11]. Soft collisions between two partons are assumed to proceed through a very low-energy double gluon exchange. This provides a natural continuation to the harder collisions above p_0, where the dominant one-gluon exchange processes in $gg \to gg$, $gq \to gq$, and $qq \to qq$ have the same overall structure [12]. A simple and physically plausible form for the soft cross-section continues the hard cross-section for Q^2 below p_0^2 down to $Q^2 = 0$ by introducing a regulating term β^2, so that we have

$$\frac{d\widehat{\sigma}_{ab\to cd}^{soft}}{dQ^2} \sim \frac{2\pi\alpha_s^2(p_0^2)}{Q^2 + \beta^2} \tag{4}$$

Thus β acts as a phenomelogical parameter which governs the overall magnitude of the integral $\sigma^{soft} \sim \ln\left[(p_0^2 + \beta^2)/\beta^2\right]$; it is estimated to be in the range of 0.3 - 1.0 GeV, and we shall use $\beta = 0.5$ GeV [2].

The only further parameter to be specified is the virtuality cut-off for the evolution of the time-like partons, below which they are assumed not to radiate; this is taken to be 1.0 GeV, as determined from fits to the hadron production in e^+e^- collisions [2]. Finally we add that the maximum possible longitudinal spread for the gluons, $\Delta z \sim 1/xP$, with P denoting the longitudinal momentum of the nucleon, is taken as 1 fm [13].

The parton cascade model provides the phase space distribution of the partons. With this given, we have the general form for the colour screening mass in the one loop approximation [3, 14]

$$\mu^2 = -\frac{3\alpha_s}{\pi^2} \lim_{|\vec{q}| \to 0} \int d^3k \frac{|\vec{k}|}{\vec{q} \cdot \vec{k}} \vec{q} \cdot \nabla_{\vec{k}} \left[f_g(\vec{k}) + \frac{1}{6} \sum_q \left\{ f_q(\vec{k}) + f_{\bar{q}}(\vec{k}) \right\} \right],$$

(5)

where α_s is the strong coupling constant, the f_i specify the phase space density of gluons, quarks, and anti-quarks and q runs over the flavour of quarks. It is easy to verify that in the case of ideal gas of massless partons, where the f_i reduce to Bose-Einstein or Fermi-Dirac distributions (with vanishing baryochemical potential μ_B), Eq. (5) reduces at high temperatures to

$$\mu^2 = 4\pi\alpha_s T^2 \left(1 + \frac{N_f}{6} \right) .$$

(6)

On the other hand, for the same system at large μ_B and low temperature, we get

$$\mu^2 = \frac{2}{\pi} \alpha_s \mu_B^2 N_f .$$

(7)

Following [3, 4], we shall assume that Eq. (5) holds also for the non-equilibrated partons created by partonic scattering and radiation in the early stages of the nuclear collision. We use the parton cascade model to estimate the phase-space density of the partons. The phase space density of the partons thus produced can be written as

$$f_i(\vec{k}) = \frac{2(2\pi)^2}{g_i V} \frac{1}{|\vec{k}|} f_i(k_T, y),$$

(8)

where g_i gives the relevant degeneracy with $g_g = 16$, and $g_q = g_{\bar{q}} = 6$, V is the volume occupied by the partons at the time τ, and k_T and y are the transverse momenta and the rapidity of the parton under consideration. The partonic distribution will be initially anisotropic with respect to the beam axis and thus the screening mass of a gluon in such a matter will depend on its direction of propagation.

It is known that the initial distribution of the partons in the parton cascade model resembles a plateau extending to rapidities $\pm Y$. Y is found to be of the order of 2 at $\sqrt{s} = 20$ A·GeV, about 3 at $\sqrt{s} = 200$ A·GeV, and more than 4–5 at energies likely to be attained at LHC. To allow a comparison of the evolving scenarios as the energy is increased, we shall keep $Y = 2$ in the following. The step-wise development of the parton-cascade in time as implemented in Monte-Carlo simulation VNI [15] is of great help in accounting for partons at some given instant of time, in a given volume. It may be noted that in the parton cascade model, the partons are given a formation-time and are counted as real particles only after this time. For ease of computation, we approximate the parton distributions as

$$f_i(k_T, y) = \frac{1}{2Y} f_i(k_T) \left[\theta(y + Y) - \theta(y - Y) \right],$$

(9)

where $f_i(k_T) = dN_i/dk_T^2$ for the partons in the volume we choose for estimating the screening mass. We are interested in seeing the variation with time τ and with distance

4

r_T in a plane transverse to the collision axis; in central collisions, the density of partons is highest along this axis. We shall therefore choose different zones $R_i < r_T < R_{i+1}$ in the central slice near $z = 0$. The screening masses in central AA collisions are then given by [3, 4]

$$\mu_T^2 = \frac{48\alpha_s}{\tau(R_{i+1}^2 - R_i^2)} \left(\frac{\sin^{-1}(\tanh Y)}{Y}\right) \int dk_T \left[\frac{1}{g_G} f_g(k_T) + \frac{1}{g_Q} \sum_f \{f_q(k_T) + f_{\bar{q}}(k_T)\}\right] \tag{10}$$

$$\mu_\parallel^2 = \mu_T^2 \left(1 + \frac{1}{\sinh Y \sin^{-1}(\tanh Y)}\right). \tag{11}$$

for the transverse and longitudinal directions, respectively. For $Y = 2$, the factor in brackets in Eq. (11) is about 1.2, so that $\mu_T \simeq \mu_\parallel$ within 10 %, and hence we shall in the remainder consider only $\mu_T \equiv \mu$.

The evolution time slice of interest is somewhat arbitrary; it can probably be fixed more precisely when discussing specific signatures, and we shall come back to this point a little further on. The calculations to be shown here will start at proper time $\tau = 0.1$ fm, assuming that at least this much time is needed to establish any kind of medium. For $\tau \geq 0.5$ fm, the screening masses tend to become only weakly time-dependent, so we present calculations up to about 1 fm.

We begin by calculating the screening mass for partonic matter in central $S - S$ collisions at SPS, RHIC, and LHC energies, for transverse distances $r_T \leq 2$ fm (Fig. 1). Here and in all subsequent calculations, the cascade starts when the two incoming nuclei are centered at $z = \pm 1$ fm and $\tau = -1$ fm. At SPS energy, the screening mass is found to be always less than 0.25 GeV and thus considerably below the deconfinement point $\mu_c \simeq 0.5$ GeV. We therefore expect that the partonic matter produced in this case could not have been deconfined. In contrast, RHIC energies bring μ just into the deconfinement zone, and for LHC, $\mu >> \mu_c$ for all times considered here, so that at the LHC, all collisions at reasonable impact parameters will lead deeply into the deconfinement regime.

Next we turn to $Pb - Pb$ collisions at the SPS, see Fig. 2. Here there is a hot center, i.e., at early times, a region for sufficiently small r_T reaches screening masses around μ_c. For $Au - Au$ collisions at RHIC (Fig. 3), μ increases by more than a factor three, so that now essentially the entire collision volume falls into the deconfined region. To study the onset of deconfinement at RHIC would thus seem to require smaller nuclei, and so we show in Fig. 4 corresponding results for $Cu - Cu$ collisions, confirming this expectation.

Before considering applications of these results to the study of deconfinement signals, we should note that our calculations are based on perturbative partonic interactions and a phenomenological extension thereof into the soft regime. There are indications [16] that non-perturbative corrections may lead to considerably larger screening masses, and it would clearly be of great interest to obtain more precise results from finite temperature lattice QCD.

For a test of deconfinement in nuclear collisions, the production and suppression of quarkonium states appears so far to be the most suitable probe [17]. The tight binding of most of these states prevents their dissociation in confined matter [18]; in a deconfined

medium, a hierarchy of suppression is predicted, governed by the size or the binding energy of the state in question [19]. In Table 1, we summarize the screening masses obtained in potential theory based on a screened confining potential [19].

State	J/ψ	χ_c	Υ	Υ'	χ_b
μ_x^{diss} (GeV)	0.70	0.34	1.57	0.67	0.56

Table 1: Critical screening masses for quarkonia.

From Fig. 2 we see that at the SPS, collisions of sufficiently heavy nuclei reach a regime in which much of the χ_c production should be suppressed by deconfinement. The effect on direct J/ψ production seems to be a more quantitative question - slight non-perturbative contributions could perhaps enhance μ enough to reach deconfinement values. In $Au - Au$ collisions at RHIC, essentially all charmonium production should be suppressed, see Fig. 3, and if sufficient statistics become possible, the onset of bottonium suppression could be studied here for the first time. The LHC, finally, would seem to be an ideal tool to carry out a systematic study of bottonium suppression.

We thus find that the effect of screening mass considerations in the parton cascade model leads to a pattern of quarkonium suppression which is very similar to what has been obtained in other, more global approaches [20]. In particular, recent suppression studies based on string [5] or parton percolation [6, 7] agree very nicely with the present results. An open question which could be addressed in the present, time-dependent approach is the dissociation of a charmonium state in an evolving medium. As a first guess, we have assumed that such states are dissociated once the screening length reaches deconfinement values. For more quantitative estimates, one should solve the bound-state problem in the presence of time-dependent screening, to see how long the nascent charmonium state has to spend in a deconfining medium before it is fully dissociated.

In closing we want to emphasize that our main aim was to outline how a microscopic evolution scheme based on parton interactions can be used to study the onset of deconfinement and its effect on deconfinement signatures. We have here used the parton cascade model; it would clearly be of interest to see if other, similar or not so similar models corroborate our results.

References

[1] K. Geiger and B. Müller, Nucl. Phys. B 369 (1992) 600.

[2] K. Geiger, Phys. Rep. 258 (1995) 376 and references there-in.

[3] T. S. Biró, B. Müller, and X.-N. Wang, Phys. Rev. Lett. B 283 (1992) 171.

[4] K. J. Eskola, B. Müller, and X.-N. Wang, Phys. Lett. B 374 (1996) 20.

[5] N. Armesto et al., Phys. Rev. Lett. 77 (1996) 3736.

[6] M. Nardi and H. Satz, Phys. Lett. B 442 (1998) 14.

[7] H. Satz, hep-ph/9908339.

[8] U. M. Heller, F. Karsch, and J. Rank, Phys. Lett. B 355 (1995) 511.

[9] J. Ellis and K. Geiger, Phys. Rev. D 52 (1995) 1500; J. Ellis and K. Geiger, Phys. Rev. D 54 (1996) 1967.

[10] N. Abou-El-Naga, K. Geiger, and B. Müller, J. Phys. G 18 (1992) 797.

[11] S. A. Bass and B. Müller, nucl-th/9908014.

[12] G. Gustafson, Z. Phys. C 15 (1982) 155.

[13] J. D. Bjorken in "Current Induced reactions", Proc. Int. Summer Institute on Theoretical Particle Physics, Hamburg 1975, J. Körner et al. (Eds.), *Lecture Notes in Physics*, Vol. 56, Springer, New York, 1976.

[14] O. K. Kalashnikov and V. V. Klimov, Sov. J. Nucl. Phys. 31 (1980) 699; V. V. Klimov, Sov. Phys. JETP 55 (1982) 199.

[15] K. Geiger, Comp. Phys. Comm. 104 (1997) 70; K. Geiger, R. Longacre, and D. K. Srivastava, nucl-th/9806102. The results reported here have been obtained using the revised version VNI/BMS by S. A. Bass, B. Müller, and D. K. Srivastava (to be published), which removes several inconsistencies in earlier versions of the code.

[16] K. Kajantie et al., Phys. Rev. Lett. 17 (1997) 3130.

[17] T. Matsui and H. Satz, Phys. Lett. B 178 (1986) 416.

[18] D. Kharzeev and H. Satz, Phys. Lett. B 334 (1994) 155.

[19] F. Karsch and H. Satz, Z. Phys. C 51 (1991) 209.

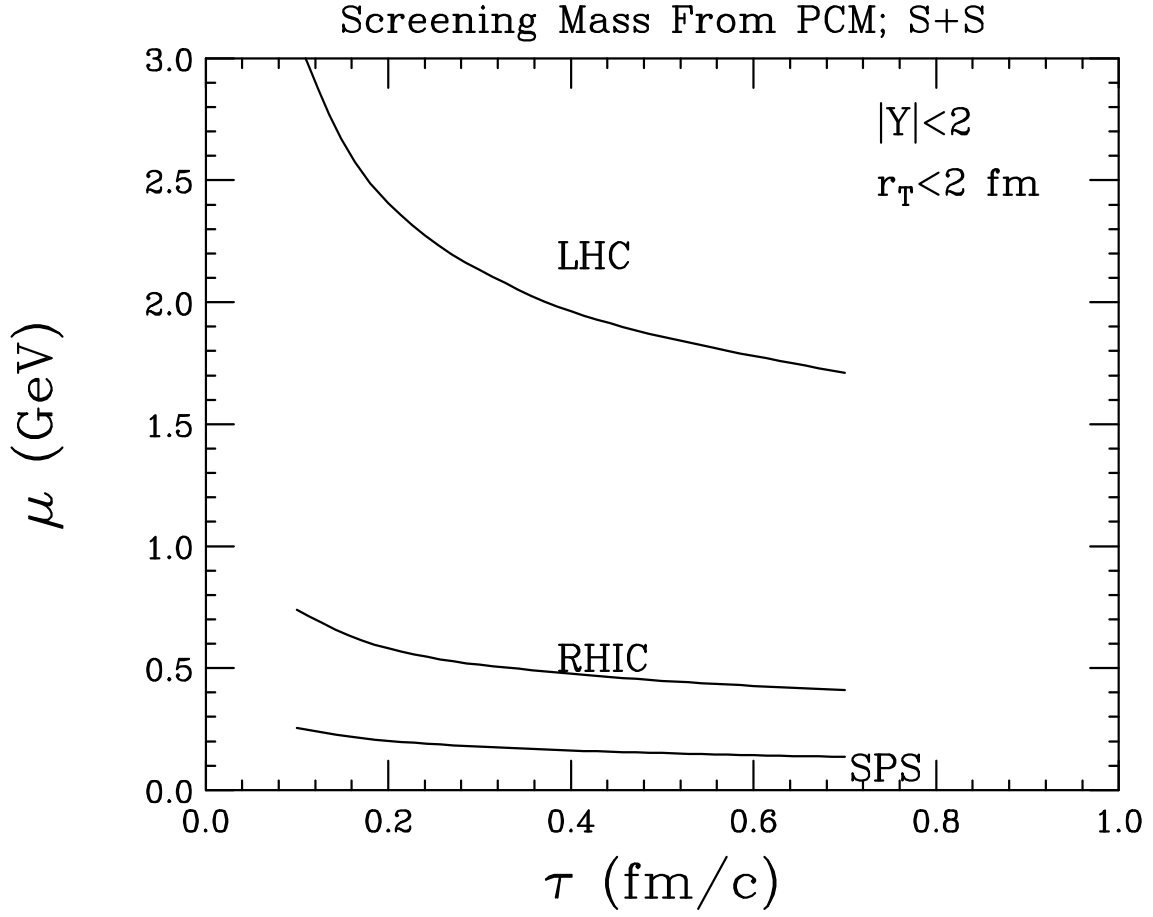[20] See e.g., D. Kharzeev and H. Satz in R. Hwa (Ed.), *Quark-Gluon Plasma 2*, World Scientific, Singapore 1995.

Figure 1: The time evolution of the colour screening mass in central $S-S$ collisions at SPS, RHIC and LHC energies.
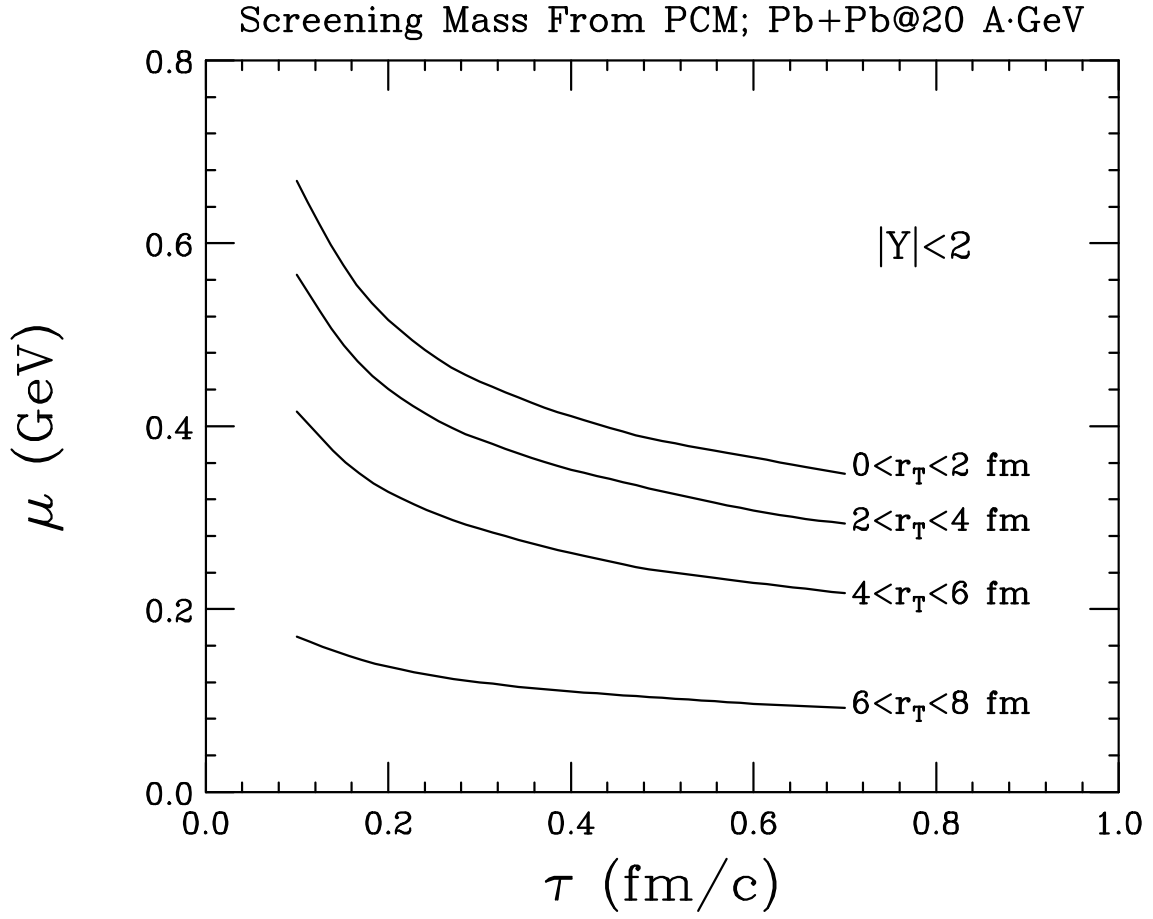
Figure 2: The time evolution of the colour screening mass in central $Pb - Pb$ collisions at SPS energy in different radial zones.
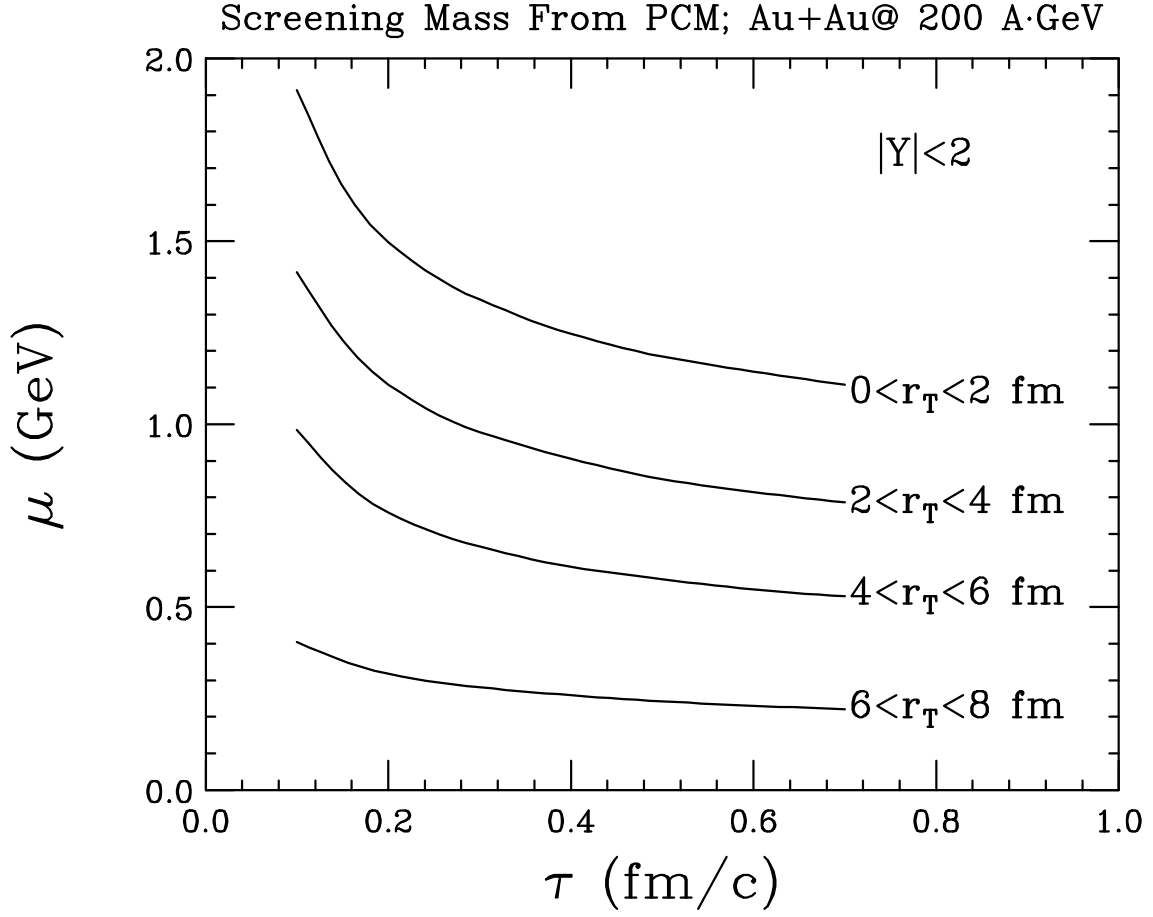
Figure 3: The time evolution of the colour screening mass in central $Au - Au$ collisions at RHIC energy in different radial zones.
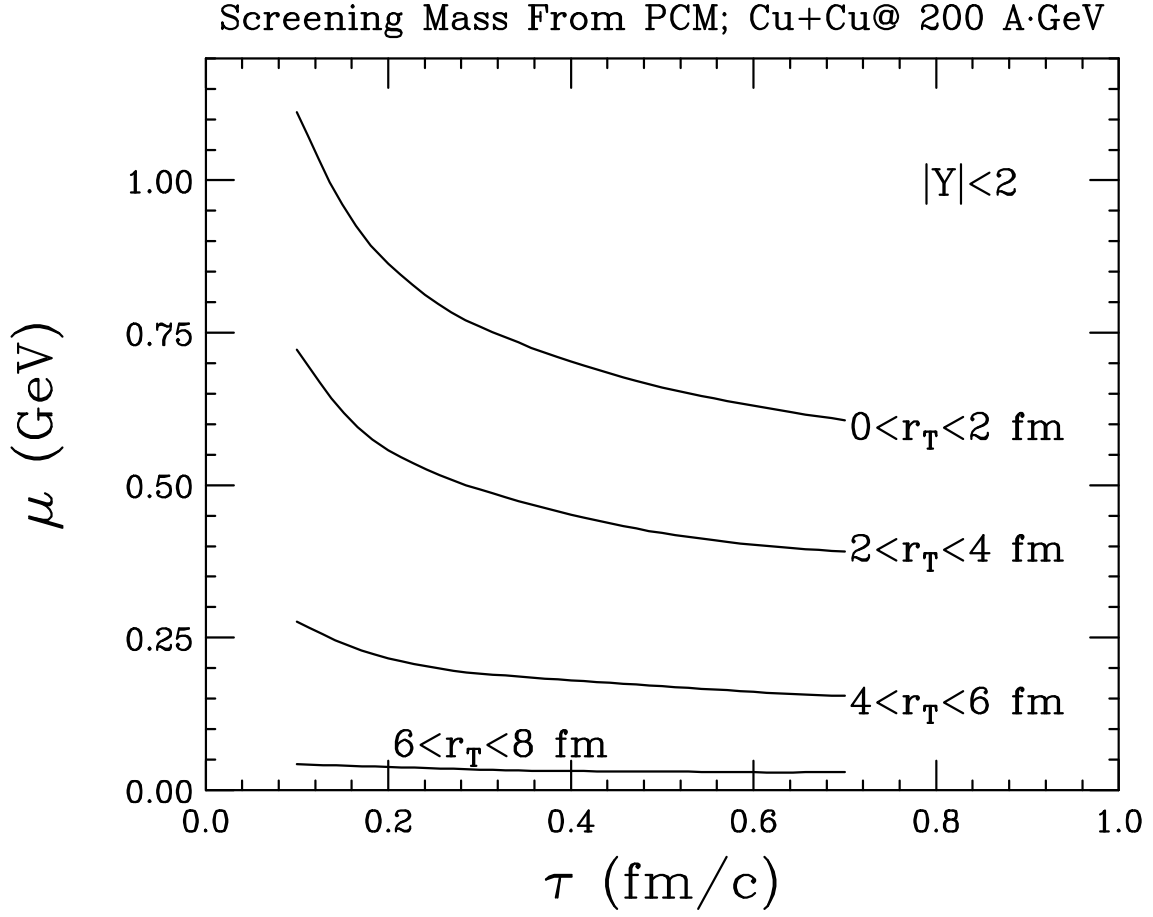
Figure 4: The time evolution of the colour screening mass in central $Cu - Cu$ collisions at RHIC energy in different radial zones.